

Article

Composite Cement Materials Based on β -Tricalcium Phosphate, Calcium Sulfate, and a Mixture of Polyvinyl Alcohol and Polyvinylpyrrolidone Intended for Osteogenesis

Kseniya Stepanova ¹, Daria Lytkina ¹, Rustam Sadykov ¹, Kseniya Shalygina ¹, Toir Khojazoda ², Rashidjon Mahmadbegov ² and Irina Kurzina ^{1,*}

¹ Faculty of Chemistry, Tomsk State University, 634050 Tomsk, Russia

² Faculty of Natural Science, Russian-Tajik (Slavonic) University, Dushanbe 734000, Tajikistan

* Correspondence: kurzina99@mail.ru; Tel.: +7-913-882-1028

Abstract: The primary purpose of the study, presented in this article, was to obtain a composite cement material intended for osteogenesis. The β -tricalcium phosphate powder (β -TCP, β -Ca₃(PO₄)₂) was obtained by the liquid-phase method. Setting and hardening of the cement system were achieved by adding calcium sulfate hemihydrate (CSH, CaSO₄·1/2H₂O). An aqueous solution of polyvinyl alcohol (PVA), polyvinylpyrrolidone (PVP), and a PVA/PVP mixture were used as a polymer component. The methods of capillary viscometry and Fourier-transform infrared spectroscopy (FTIR) revealed the formation of intermolecular hydrogen bonds between polymer components, which determines the good miscibility of polymers. The physicochemical properties of the synthesized materials were characterized by X-ray diffraction (XRD) and FTIR methods, and the added amount of polymers does not significantly influence the processes of phase formation and crystallization of the system. The size of crystallites CSD remained in the range of 32–36 nm, regardless of the ratio of polymer components. The influence of the composition of composites on their solubility was investigated. In view of the lower solubility of pure β -TCP, as compared to calcium sulfate dihydrate (CSD, CaSO₄·2H₂O), the solubility of composite materials is determined to a greater degree by the CSD solubility. Complexometric titration showed that the interaction between PVA and PVP impeded the diffusion of calcium ions, and at a ratio of PVA to PVP of 1/1, the smallest exit of calcium ions from the system is observed. The cytotoxicity analysis results allowed us to establish the fact that the viability of human macrophages in the presence of the samples varied from 80% to 125% as compared to the control.

Keywords: bone cement; composite; β -TCP; PVA; PVP



Citation: Stepanova, K.; Lytkina, D.; Sadykov, R.; Shalygina, K.; Khojazoda, T.; Mahmadbegov, R.; Kurzina, I. Composite Cement Materials Based on β -Tricalcium Phosphate, Calcium Sulfate, and a Mixture of Polyvinyl Alcohol and Polyvinylpyrrolidone Intended for Osteogenesis. *Polymers* **2023**, *15*, 210. <https://doi.org/10.3390/polym15010210>

Academic Editors: José Miguel Ferri, Vicent Fombuena Borràs and Miguel Fernando Aldás Carrasco

Received: 3 December 2022

Revised: 26 December 2022

Accepted: 29 December 2022

Published: 31 December 2022



Copyright: © 2022 by the authors. Licensee MDPI, Basel, Switzerland. This article is an open access article distributed under the terms and conditions of the Creative Commons Attribution (CC BY) license (<https://creativecommons.org/licenses/by/4.0/>).

1. Introduction

The development of new biomaterials for bone tissue restoration is a relevant topic in the field of regenerative medicine [1]. This trend is conditioned by the prevalence of bone tissue defects resulting from fractures, infectious and tumor processes, age-related osteoporosis, and some other pathological conditions of the bone. Bone tissue regeneration is a limited and time-consuming process; therefore, it is necessary to use bone substitutes [2]. In addition, serious disadvantages of natural bone grafts are known: An autograft requires additional surgical interventions and does not exclude the probability of donor site morbidity, and an allograft can cause tissue rejection and transmit infections [3].

Bone cement can be defined as a family of materials consisting of powder and liquid phases that, after mixing, form a plastic paste that can self-cure once implanted into the body. This means that the material is moldable, which ensures a perfect fit to the implant site and good bone-to-material contact, even in geometrically complex defects [4]. Recent advances in orthopedic surgery are associated with the use of minimally invasive surgical techniques. In this area, it is critical to have injectable materials available, and in this

sense, bone cement can play a decisive role, provided that injectable cement is developed. An example is the performance of some minimally invasive surgical procedures, namely vertebroplasty and kyphoplasty, to repair vertebral compression fractures, in which bone cement is injected into the vertebral body [4].

Improving the properties of bone cement can be achieved by reinforcing the cement matrix with either particles or fibers [5–10]. In some cases, the addition of water-soluble polymers can be used to change the adhesion of the cement slurry or its rheological properties. For construction cement, there is evidence that the combined use of sulfates and polyvinyl alcohol adversely affects the strength of cement [11]. However, for bone cement, there are studies confirming that the addition of certain water-soluble polymers can be very effective in improving the adhesion of bone cement pastes [12,13].

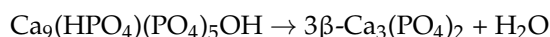
Of the many biomaterials, synthetic calcium phosphates (CaP) have proven themselves in a number of studies because of their chemical similarity to the bone mineral component [14,15]. CaP is used in the form of ceramic products [16,17], coatings on metal implants [18], or in the form of cement pastes [19,20]. Bone cement is characterized by a paste-like consistency, set at the body temperature, which allows molding the implant at the site of the defect with a firm adherence to the surrounding tissues, as well as using a minimally invasive technique of a surgical operation by means of injection [21–26].

Among CaP, hydroxyapatite (HA, $\text{Ca}_{10}(\text{PO}_4)_6(\text{OH})_2$) and tricalcium phosphate (TCP, $\text{Ca}_3(\text{PO}_4)_2$) have become preferable for bone tissue regeneration [3,27–30]. Based on published results [15,31], β -TCP tends to have higher osteoconductivity as compared to that of HA and α -TCP. HA has been reported to behave similarly to an inert implant [32], while β -TCP is moderately dissolved as a result of cell-mediated resorption [33–37]. The main disadvantage of α -TCP is that the resorption rate is too fast [38]. The research results in [39] show that β -TCP is an excellent material with respect to stem cell differentiation and in vivo osteoinduction compared to pure HA and an HA/TCP mixture.

We selected a β -TCP-based material for the study. The cement powder was obtained by adding calcium sulfate (CS), which has been used as an orthopedic biomaterial for many years [40–42]. In [43], the effect of the CS/ β -TCP composite was studied as compared to that of β -TCP with the example of treating iliac bone defects occurring in dogs. Four months later, CS/ β -TCP demonstrated a much greater contribution to the new bone formation as opposed to that of pure β -TCP. The addition of medical gypsum will allow for obtaining a material with selective resorption, where the calcium-phosphate matrix acts as a relatively stable framework and CS acts as a pore-former and setting component. The inclusion of biocompatible polymers in the cement formulation will allow the most complete imitation of the natural matrix of the bone tissue and improve the mechanical properties of the material. Polyvinyl alcohol (PVA) and polyvinylpyrrolidone (PVP) are suitable biodegradable and nontoxic polymers [44,45], and a mixture based on them improves the in vivo stability of polymers, that is, it allows for preventing the PVA suspension formation under physiological conditions [30].

2. Materials and Methods

β -TCP was synthesized by the liquid-phase method at a pH of 11 according to the following equations:



Solutions of calcium nitrate $\text{Ca}(\text{NO}_3)_2$ 1.2 M and ammonium hydrophosphate $(\text{NH}_4)_2\text{HPO}_4$ 0.8 M were prepared separately at room temperature (25 °C). $\text{Ca}(\text{NO}_3)_2$ and $(\text{NH}_4)_2\text{HPO}_4$ were purchased from Sigma-Aldrich (MO, USA). The initial reagents were taken in equimolar volumes so that the molar ratio of Ca/P elements was 3/2. The $\text{Ca}(\text{NO}_3)_2$ solution was added dropwise to the $(\text{NH}_4)_2\text{HPO}_4$ solution while stirring on a magnetic stirrer. pH 11 was maintained by adding a concentrated ammonia solution (35%).

Next, to establish the effect of mixing time on the phase composition of the phosphate, half of the suspension continued to be stirred for 12 h; in the case of the second half of the suspension, the next synthesis step immediately began. The white precipitate was washed with distilled water and isopropyl alcohol. The suspension was subjected to vacuum filtration. The formed precipitate was dried at 80 °C for a day. The dried powder was crushed and then calcined at 900 °C for two hours to form the TCP beta phase. In the first part, after mixing, all the same operations were performed.

PVA (with an average molecular weight of 104,500 g/mol) was purchased from Sigma Aldrich (Saint Louis, MO, USA). PVP (with a molecular weight of 3500 g/mol) was provided by Acros Organics (Geel, Belgium). The PVA 5 wt% solution was prepared in distilled water at 90 °C during constant mixing with a magnetic stirrer for 1 h. The aqueous PVP 5 wt% solution was prepared at room temperature during constant stirring for 15 min. The PVA/PVP 5 wt% mixture was prepared by mixing freshly prepared solutions in the ratios of 1/3, 1/1, and 3/1.

The minimum amount of medical gypsum required for setting the β -TCP-based cement was selected experimentally. For this reason, calcium sulfate hemihydrate (CSH, $\text{CaSO}_4 \cdot 1/2\text{H}_2\text{O}$) was mixed in amounts of 50, 40, 30, 20, and 10 wt% with β -TCP and water in a powder-to-liquid ratio of 1/1. When adding 30 wt% of gypsum, the setting was noticeable, whereas, at 20 and 10 wt%, the consistency was still quite liquid. The following powder composition was chosen: 30 wt% of CSH and 70 wt% of β -TCP.

Composite cement materials were obtained by direct mechanical mixing of β -TCP/CSH powder components with the addition of pure water and the PVA, PVP, and PVA/PVP solutions in the ratios of 1/3, 1/1, and 3/1. The powder and liquid were mixed in a ratio of 1/1. The synthesis was carried out in Petri dishes. The setting time of the samples varied from 7 to 10 min. The obtained cement paste was left to harden completely.

The phase composition of the initial components and composites was determined using a MiniFlex 600 diffractometer (Rigaku). The survey photographing of the samples was performed under monochromatic $\text{CuK}\alpha$ ($\alpha = 1.5418 \text{ \AA}$) radiation in the reflection angular range of $2\theta = 5\text{--}100^\circ$ in increments of 0.02° , with a voltage of 40 kV and a speed of $3^\circ/\text{min}$. The phases were decoded and identified using the ICDD diffraction database (PDF-2/Release 2012 RDB). To calculate the coherent scattering region (CSR), the reflex value at its half-height was determined using the Gaussian function in Origin software.

The spectra of the surface layer of the samples were recorded by means of the Nicolet 6700 IR-Fourier spectrometer (Thermo Scientific). The spectra were recorded with a resolution of 4 cm^{-1} in the range of $400\text{--}4000 \text{ cm}^{-1}$, using the FTIR attachment.

The 5 wt% solution viscosity of the PVA/PVP mixture, depending on the mixing time of the solutions, was measured at room temperature using a capillary viscometer ($d = 1.31 \text{ mm}$).

To determine the solubility, the samples were soaked in the physiological solution at 37 °C for 20 days. The total weight loss of the samples and the total concentration of calcium ions in the solution were recorded every 5 days.

The weight losses were calculated as a percentage using the formula:

$$\text{Losses, wt\%} = (m_i - m_k) \cdot 100\% / m_i$$

where m_i is the initial weight of the sample and m_k is the sample weight after soaking the sample in distilled water.

The Ca^{2+} concentration in the solution was determined by complexometric titration in the presence of Eriochrome Black T and the ammoniac buffer solution with a pH of 10.

The viability of immune system cells on the surface of the studied materials was assessed using the Alamar Blue indicator. The optical density was measured using a Tecan Infinite 200 microreader at wavelengths of 573 and 605 nm.

The data were analyzed using Student's t -test and presented as an average \pm standard deviation. Three duplicate samples were used in all the experiments. The data probability was considered statistically significant for values of $p < 0.05$.

3. Results and Discussion

The X-ray diffraction (XRD) measurement results allowed us to establish that the sample (Figure 1a), left to mix for 12 h, contained two phases: A major β -TCP and a hydroxyapatite (HA) admixture. At the same time, the sample (Figure 1b) obtained without mixing contained the third phase: Beta-form calcium pyrophosphate (β -Ca₂P₂O₇). In this way, such mixing influences the phase formation process of calcium phosphate. The appearance of HA and β -Ca₂P₂O₇ admixtures may be caused by an inhomogeneous distribution of the components in the solution during the deposition of β -Ca₃(PO₄)₂ [43]. HA forms at a temperature of approximately 900 °C in air, most likely via HA dehydroxylation [46]. We selected sample (a) for further work.

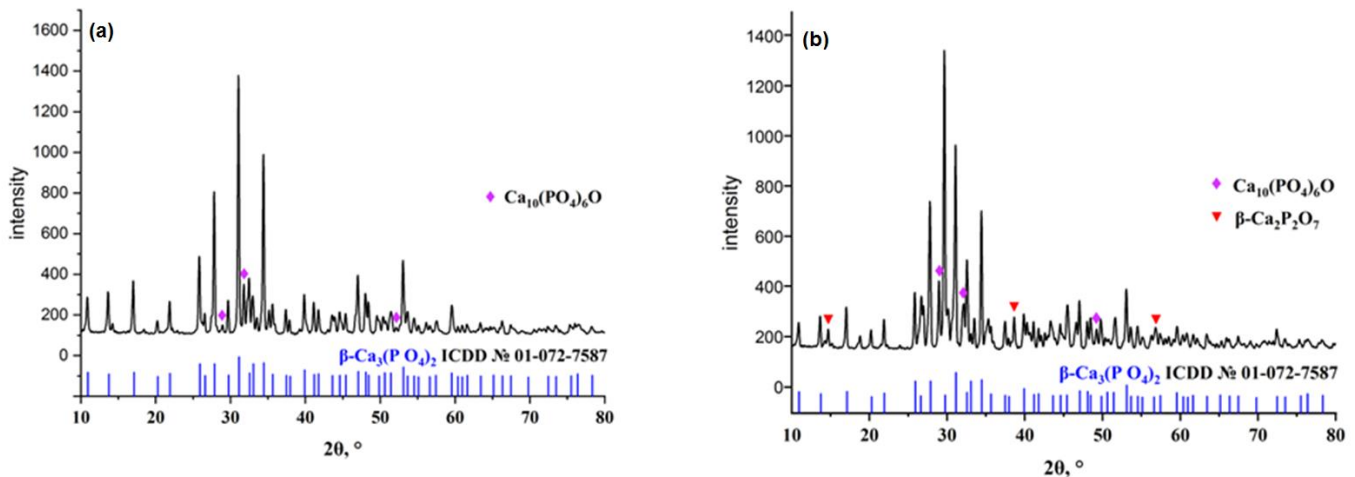


Figure 1. Sample left to mix for 12 h: (a) β -Ca₃(PO₄)₂, (b) Ca₁₀(PO₄)₆O.

According to the XRD data, at different ratios of the polymers, the composite samples are characterized by the same phase composition: β -Ca₃(PO₄)₂, CaSO₄·2H₂O, Ca₁₀(PO₄)₆O (Figure 2).

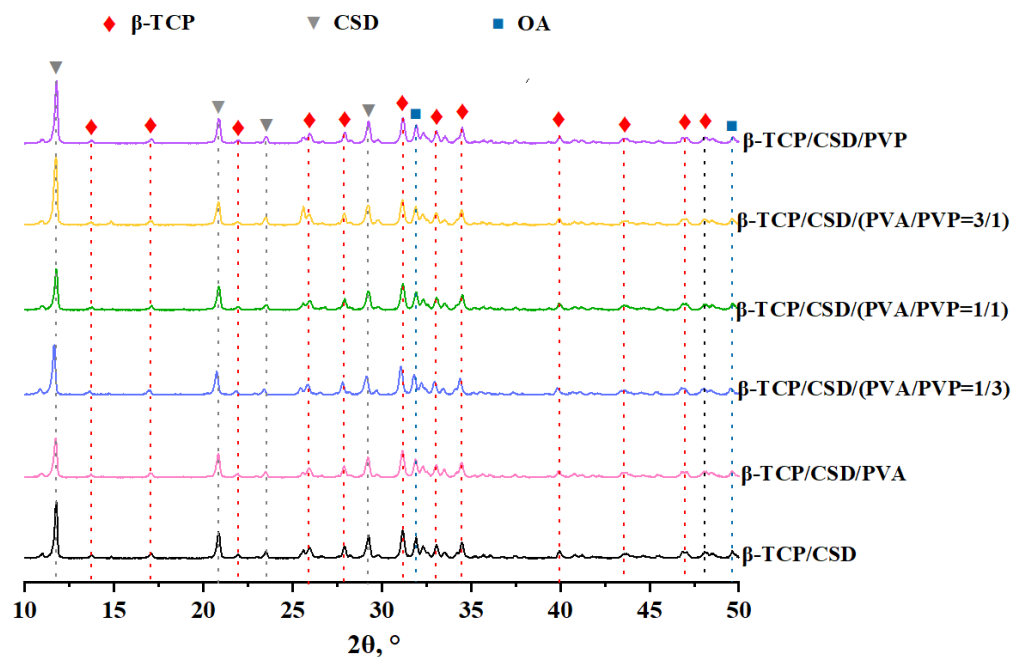


Figure 2. Diffraction patterns of composite cement materials.

The size of the crystallites in the composite cement samples varied in the range of 28–31 nm and 32–36 nm for the β - $\text{Ca}_3(\text{PO}_4)_2$ and $\text{CaSO}_4 \cdot 2\text{H}_2\text{O}$ phases, respectively (Table 1), i.e., there is a fairly uniform distribution of phases by the size of the crystallites. The CSR values for the β - $\text{Ca}_3(\text{PO}_4)_2$ phase, included in the initial CaP and part of the composites, essentially do not change. In the case of CSH, the size of the crystallites is somewhat smaller than that of CSD included in the composites, since hydration occurs when mixing with water. Then, calcium sulfate dihydrate microcrystals grow in size, intertwine, and grow together. As a result, the addition of polymers does not significantly influence the processes of phase formation and crystallization of the system.

Table 1. CSR values of cement and initial powder components.

Sample	CSR Values for Different Phases, nm		
	β -TCP	CSD	CSH
β -TCP	30	—	—
CSH	—	—	28
β -TCP/CSD	31	36	—
β -TCP/CSD/PVA	30	34	—
β -TCP/CSD/(PVA/PVP = 1/3)	29	32	—
β -TCP/CSD/(PVA/PVP = 1/1)	28	33	—
β -TCP/CSD/(PVA/PVP = 3/1)	33	36	—
β -TCP/CSD//PVP	28	32	—

The Fourier-transform infrared spectroscopy (FTIR) method was used to study films of the 5% aqueous solutions of PVA, PVP, and PVA/PVP. Figure 3 shows the fundamental absorption bands of functional groups. The following specific bands were found for pure PVA [47,48]. A wide band of approximately 3343 cm^{-1} corresponds to the valence vibration of the νOH hydroxyl group. Two bands are observed at 2930 cm^{-1} and 2908 cm^{-1} , corresponding to the asymmetric and symmetric valence vibrations of νCH_2 , respectively. The bands at 1418 cm^{-1} and 828 cm^{-1} are related to the scissor vibration of δCH_2 and stretching of the zigzag-shaped carbon base of $\nu\text{C-C}$, respectively. The absorption band at 1323 cm^{-1} characterizes the deformation vibrations of $\delta(\text{CH}+\text{OH})$. The wagging vibration of δCH is poorly observed at 1237 cm^{-1} . The absorption of approximately 1084 cm^{-1} corresponds to the stretching of the acetyl groups of $\nu\text{C-O}$ that are present in the main PVA chain. The weak band at 916 cm^{-1} can be referred to as the rocking vibration of δCH_2 .

The following specific bands were found for pure PVP [47–51]. The observed wide low-intensity band of approximately 3468 cm^{-1} is related to the stretching of the OH-group of the water adsorbed on the polymer surface. The absorption band at 2951 cm^{-1} corresponds to the asymmetrical vibration of νCH_2 . The bands at 1421 cm^{-1} and 840 cm^{-1} correspond to the scissor vibrations of δCH_2 and the chain bending of $\nu\text{C-C}$, respectively. The bands at 1657 cm^{-1} and 1284 cm^{-1} can be referred to as valence vibrations of the $\nu\text{C=O}$ carbonyl group and the stretching of the group of the $\nu\text{C-N}$ pyrrolidone ring, respectively.

The participation of the hydroxyl group in the formation of intermolecular hydrogen bonds is manifested through the shift of the absorption band towards lower frequencies and a significant increase in its intensity [51]. The absorption band of the PVA hydroxyl group at 3343 cm^{-1} shifts towards lower wave numbers at 3313 cm^{-1} for the PVA/PVP mixture due to the formation of an intermolecular hydrogen bond between the PVP carbonyl group and the PVA hydroxyl group [40]. At the same time, a slight shift of the absorption band of the electron donor group by $10\text{--}20\text{ cm}^{-1}$ is characteristic [51]; therefore, the PVP carbonyl band group is shifted from 1656 cm^{-1} to 1649 cm^{-1} .

The IR spectra peculiarity of CaP is the presence of two doubled absorption bands. The first is detected at wave numbers such as $\nu = 900\text{--}1200\text{ cm}^{-1}$ and the second at $\nu = 350\text{--}650\text{ cm}^{-1}$ [52]. Figure 4 shows that the vibrations of the β -TCP phosphate groups are located at approximately 550 and 1020 cm^{-1} .

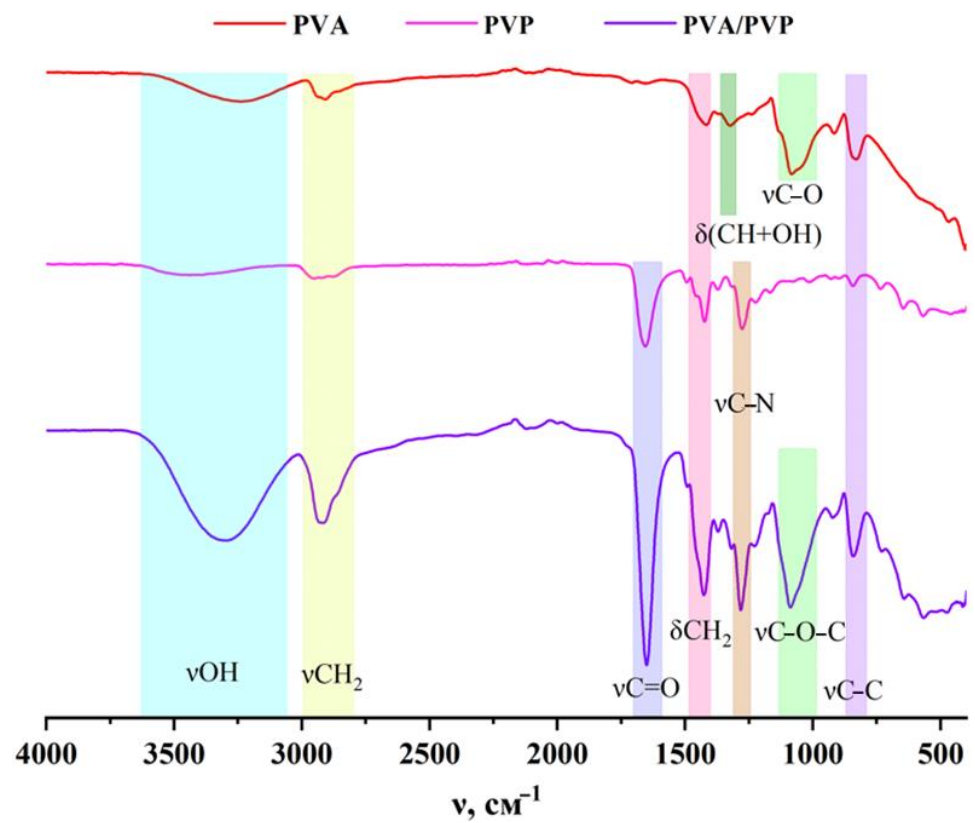


Figure 3. IR-spectrum of the 5% aqueous solutions of PVA, PVP, and PVA/PVP.

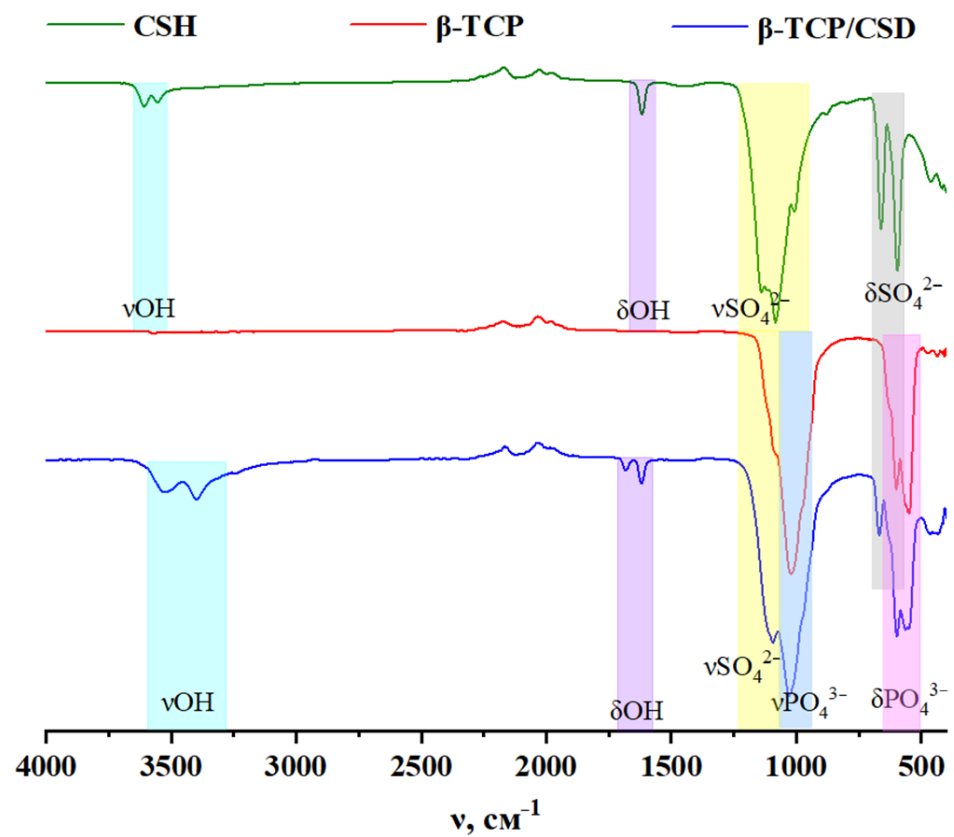


Figure 4. IR spectrum of CSH, β -TCP, and β -TCP/CSD water cement.

In the IR spectrum of β -TCP/CSD, there is a slight shift of the bands of valence vibrations of the νPO_4^{3-} groups to a longer wavelength region due to the formation of a new phase on phosphate particles and anion geometry distortion as a result of nonsymmetric interactions in the crystal. Specific absorption bands are also observed at 3400 cm^{-1} and 1620 cm^{-1} , which are related to the adsorbed water (bound OH-group), its valence, and deformation vibrations, respectively. The band at 3527 cm^{-1} appears because of the valence vibrations of OH-ions of the crystallohydrate lattice (free OH-group) [30].

The sulfate ion can be identified by valence and deformation vibrations in the range of $980\text{--}1100\text{ cm}^{-1}$ and $550\text{--}650\text{ cm}^{-1}$, respectively [52]. In the case of $\text{CaSO}_4 \cdot 1/2\text{H}_2\text{O}$, there are fluctuations in the sulfate and hydroxide ions of the lattice, as shown in Figure 4.

The IR spectra of the composites (Figure 5) differ by the small shifts of the sulfate group band, which may be related to anion geometry distortion, inductive, and mesomeric effects as a result of the interaction with polymeric chains.

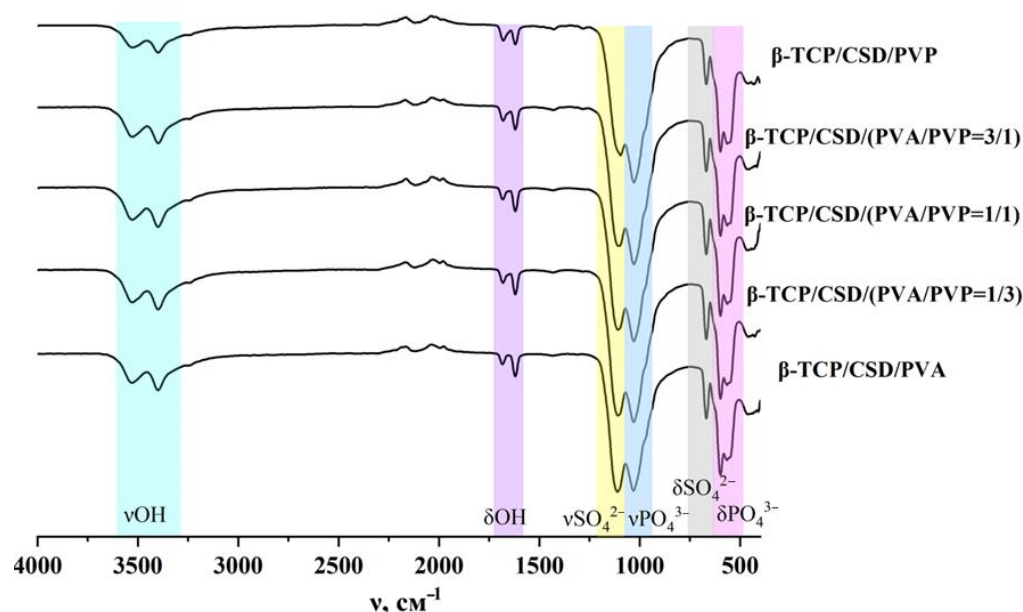


Figure 5. IR spectra of composite cement materials.

A graph was constructed based on the capillary viscometry results (Figure 6). In the first 30–40 min of mixing the polymers, the relative viscosity increases significantly. These results can be explained by the interaction between PVP and PVA, conditioned by the formation of intermolecular hydrogen bonds between the carbonyl group of the pyrrolidone ring and the side hydroxyl PVA group.

A series of experiments were conducted to study the solubility of the samples. The data in Table 2 demonstrate that the weight losses of cement materials increased along with an increase in the soaking time of the samples. In view of the lower solubility of pure β -TCP as compared to CSD, the solubility of the composite materials is more determined by the CSD solubility. In the case of the composites, weight losses varied in the range of 68 to 76 wt%, while in the occasion of pure β -TCP, the losses reached only 47 wt%.

In the case of the composites containing a mixture of polymers, the release of calcium ions is lower than that in the composites containing only one polymer (Figure 7). The interaction between PVA and PVP manifests itself in a solution viscosity increase, which hinders the diffusion of calcium ions.

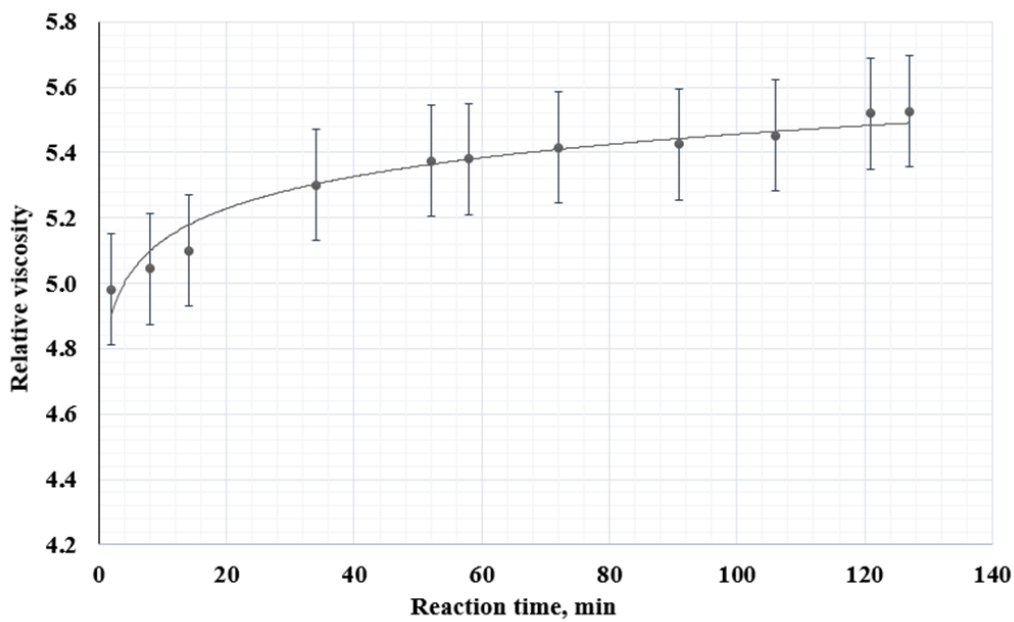


Figure 6. Relative viscosity measurement of the 5% solution of the PVA/PVP mixture.

Table 2. Weight losses of the composites and the initial β -TCP depending on the duration of sample soaking in the physiological solution.

Number of Days	β -TCP	Weight Losses, wt%					
		β -TCP/CSD	β -TCP/CSD/PVA	β -TCP/CSD/ (PVA/PVP = 1/3)	β -TCP/CSD/ (PVA/PVP = 1/1)	β -TCP/CSD/ (PVA/PVP = 3/1)	β -TCP/ CSD/PVP
5	33	34	54	63	60	47	34
10	40	48	62	65	64	60	40
15	46	67	75	67	69	72	69
20	47	68	76	70	72	76	69

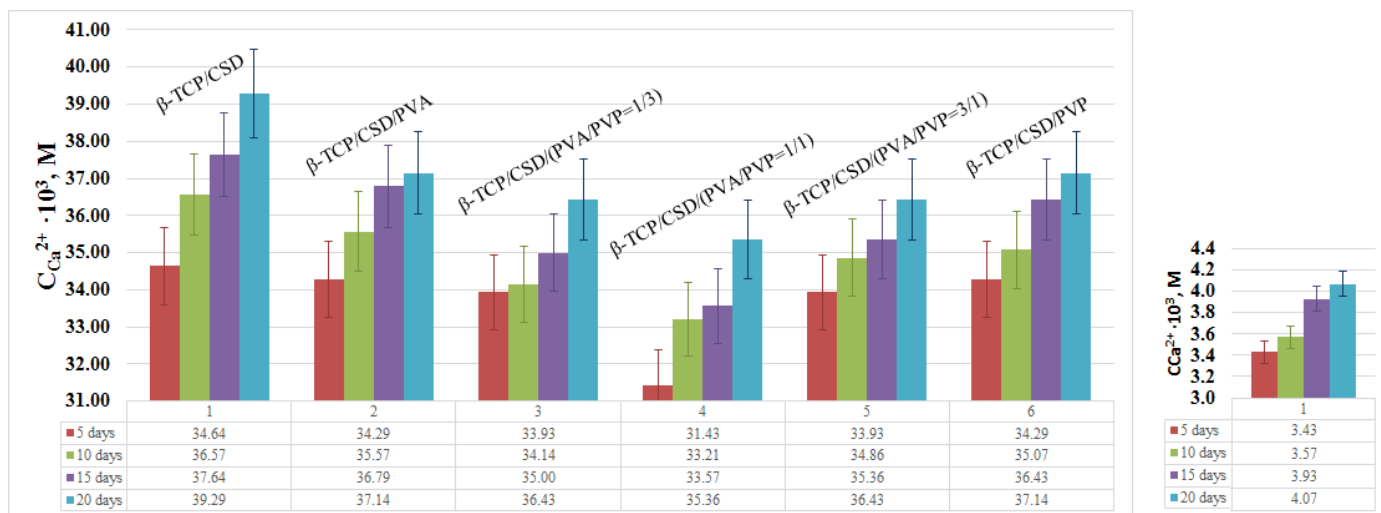


Figure 7. Release of Ca^{2+} ions within 20 days for the composites and the initial β -TCP.

The studies conducted on human macrophages (Figure 8) have shown that, in the presence of the samples, most of the cells do not die. The viability of monocytes varies from 80% to 125% as compared to the control (100%).

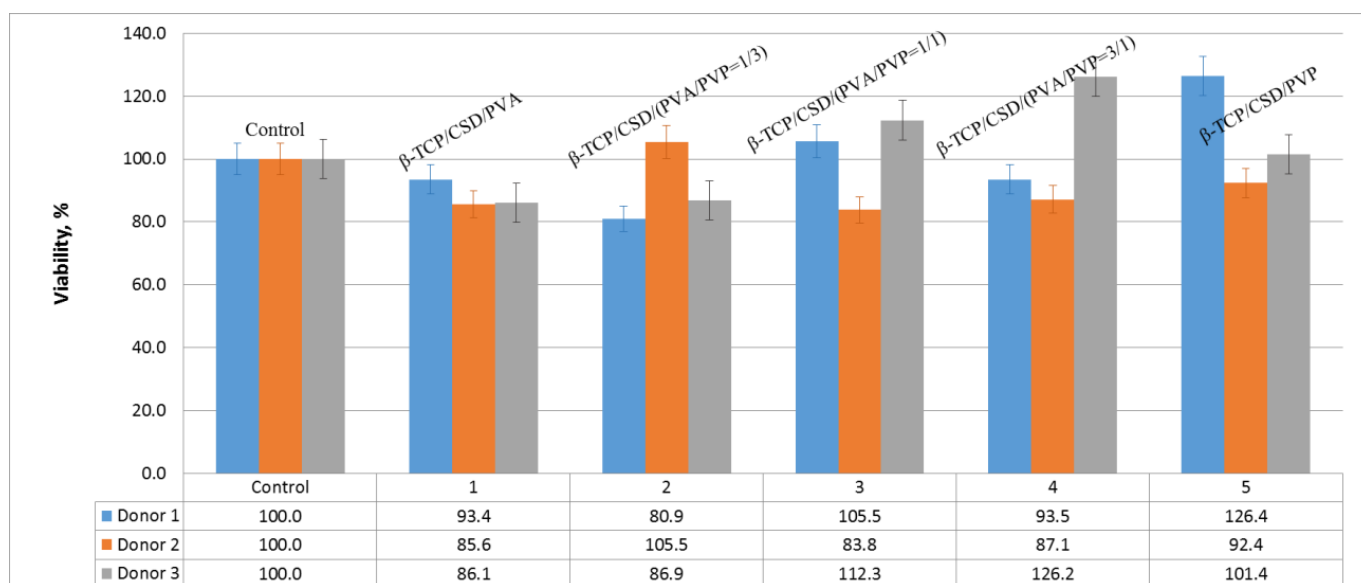


Figure 8. Viability of human macrophages in the presence of composite cement.

Within the series, there is no unique dependence of cytotoxicity on different concentration ratios of polymers in the cement composition. Comparing the composites with individual polymers, it is possible to state that cell viability is higher in the presence of PVP, which confirms its hemocompatibility. It is also possible to observe that some donors have an individual reaction to the material: Donor 2 shows lower viability relative to other samples, which suggests that the viability of monocytes in the presence of materials is comparable to the control or higher. The fact that more cells survive in some donors than in controls indicates that the environment in the presence of materials is more favorable and more cells survive after incubation. From parallel studies [53] involving hydroxyapatite and polyvinyl alcohol-based gels, we know that PVA supplementation can significantly improve macrophage survival. In the case of bone cement, we observe the same effect. Thus, it can be assumed that the co-administration of polymers has a beneficial effect on the viability of macrophages, which shows the possibility of further development of these studies, which may consist of finding a narrower range of effective concentrations of the components, as well as establishing and improving mechanical characteristics.

4. Conclusions

1. In this work, a number of composite cement materials based on β -TCP and CSD were obtained and characterized with the addition of PVA and PVP solutions and a PVA/PVP mixture solution in the ratios of 1/3, 1/1, and 3/1.
2. The selected polymers mix well with each other and form a stable homogeneous solution. The formation of intermolecular hydrogen bonds between the polymer components was detected by capillary viscometry and IR-spectroscopy.
3. According to the XRD results, the added amount of polymers does not significantly influence the processes of phase formation and crystallization of the system.
4. It has been found that the solubility of the cement is determined to a greater extent by the CSD solubility in view of the lower solubility of pure β -TCP. The manifested interaction between the polymeric components hinders the diffusion and release of calcium ions.
5. The study of the cytotoxicity level of the composite cement materials has shown that most of the cells do not die in the presence of the samples. Consequently, these composites are very promising biomaterials for bone regeneration.

Author Contributions: Conceptualization, I.K.; methodology, I.K.; investigation, K.S. (Kseniya Stepanova), R.S. and K.S. (Kseniya Shalygina); writing—original draft preparation, K.S. (Kseniya Stepanova), D.L., I.K. and R.M.; writing—review and editing, D.L. and T.K. All authors have read and agreed to the published version of the manuscript.

Funding: Synthesis and studies of the phases and solubility of calcium phosphates were supported by grants from the President of the Russian Federation for state support of young Russian scientists-PhDs (MK-2182.2022.1.3). The study of IR spectra, degradation, and in vitro studies were supported by the Tomsk State University Development Programme (Priority-2030).

Institutional Review Board Statement: The study was conducted according to the guidelines of the Declaration of Helsinki and approved by the Ethics Committee of Tomsk State University (Protocol of the meeting of NR TSU Bioethics Commission, Protocol No 3 from 7 March 2022). Informed consent was obtained from all subjects involved in the study. Written informed consent has been obtained from the patient to publish this paper.

Informed Consent Statement: Not applicable.

Data Availability Statement: All data presented in this study are contained within the article.

Conflicts of Interest: The authors declare no conflict of interest.

References

1. Pina, S.; Oliveira, J.M.; Reis, R.L. Natural-based nanocomposites for bone tissue engineering and regenerative medicine: A review. *Adv. Mater.* **2015**, *27*, 1143–1169. [[CrossRef](#)] [[PubMed](#)]
2. Sun, X.; Su, W.; Ma, X.; Zhang, H.; Sun, Z.; Li, X. Comparison of the osteogenic capability of rat bone mesenchymal stem cells on collagen, collagen/hydroxyapatite, hydroxyapatite and biphasic calcium phosphate. *Regen. Biomater.* **2018**, *5*, 93–103. [[CrossRef](#)]
3. Kucko, N.W.; Herber, R.P.; Leeuwenburgh, S.C.; Jansen, J.A. Calcium phosphate bioceramics and cements. In *Principles of Regenerative Medicine*, 3rd ed.; Academic Press: London, UK, 2019; pp. 591–611.
4. Ginebra, M.-P.; Montufar, E.B. Cements as bone repair materials. In *Bone Repair Biomaterials*; Woodhead Publishing: Cambridge, UK, 2019; pp. 233–271.
5. Guida, G.; Riccio, V.; Gatto, S.; Migliaresi, C.; Nicodemo, L.; Nicolais, L.; Palomba, C. *Biomaterials and Biomechanics*; Elsevier Science: Amsterdam, The Netherlands, 1984; Volume 19.
6. Henning, W.; Blencke, B.A.; Brömer, H.; Deutscher, K.K.; Gross, A.; Ege, W. Investigations with bioactivated polymethylmethacrylates. *J. Biomed. Mater. Res.* **1979**, *13*, 89–99. [[CrossRef](#)] [[PubMed](#)]
7. Murakami, A.; Behiri, J.C.; Bonfield, W. Rubber-modified bone cement. *J. Mater. Sci.* **1988**, *23*, 2029–2036. [[CrossRef](#)]
8. Liu, Y.K.; Park, J.B.; Njus, G.O.; Steinstra, D. Bone particle impregnated bone cement: In vitro studies. *J. Biomed. Mater. Res.* **1987**, *21*, 247–261. [[CrossRef](#)]
9. Henrich, D.E.; Cram, A.E.; Park, J.B.; Liu, Y.K.; Reddi, H. Inorganic bone and demineralized bone matrix impregnated bone cement: A preliminary in vivo study. *J. Biomed. Mater. Res.* **1993**, *27*, 277–280. [[CrossRef](#)]
10. Topoleski, L.D.T.; Ducheyne, P.; Cuckler, J.M. The fracture toughness of titanium fibre reinforced bone cement. *J. Biomed. Mater. Res.* **1992**, *26*, 1599–1617. [[CrossRef](#)]
11. Haider, M. Al-Baghdadi Experimental study on sulfate resistance of concrete with recycled aggregate modified with polyvinyl alcohol (PVA). *Case Stud. Constr. Mater.* **2021**, *14*, e00527.
12. Ishikawa, K.; Miyamoto, Y.; Kon, M.; Nagayama, M.; Asaoka, K. Non-decay type fast-setting calcium phosphate cement: Composite with sodium alginate. *Biomaterials* **1995**, *16*, 527–532. [[CrossRef](#)]
13. Khairoun, I.; Boltong, M.G.; Driessens, F.C.; Planell, J.A. Effect of calcium carbonate on clinical compliance of apatitic calcium phosphate bone cement. *J. Biomed. Mater. Res.* **1997**, *38*, 356–360. [[CrossRef](#)]
14. Cama, G. *Calcium Phosphate Cements for Bone Regeneration. Biomaterials for Bone Regeneration*; Woodhead Publishing: Cambridge, UK, 2014; pp. 3–25.
15. Tang, Z.; Li, X.; Tan, Y.; Fan, H.; Zhang, X. The material and biological characteristics of osteoinductive calcium phosphate ceramics. *Regen. Biomater.* **2018**, *5*, 43–59. [[CrossRef](#)] [[PubMed](#)]
16. Wang, Y.; Li, X.; Luo, Y.; Zhang, L.; Chen, H.; Min, L.; Chang, Q.; Zhou, Y.; Tu, C.; Zhu, X.; et al. Application of osteoinductive calcium phosphate ceramics in giant cell tumor of the sacrum: Report of six cases. *Regen. Biomater.* **2022**, *9*, rbac017. [[CrossRef](#)] [[PubMed](#)]
17. Tian, P.; Liu, X. Surface modification of biodegradable magnesium and its alloys for biomedical applications. *Regen. Biomater.* **2015**, *2*, 135–151. [[CrossRef](#)] [[PubMed](#)]
18. Meng, D.; Dong, L.; Yuan, Y.; Jiang, Q. In vitro and in vivo analysis of the biocompatibility of two novel and injectable calcium phosphate cements. *Regen. Biomater.* **2019**, *6*, 13–19. [[CrossRef](#)]
19. Wang, P.; Song, Y.; Weir, M.D.; Sun, J.; Zhao, L.; Simon, C.G.; Xu, H.H. A self-setting iPSMSC-alginate-calcium phosphate paste for bone tissue engineering. *Dent. Mater.* **2016**, *32*, 252–263. [[CrossRef](#)]

20. Low, K.L.; Tan, S.H.; Zein, S.H.S.; Roether, J.A.; Mourino, V.; Boccaccini, A.R. Calcium phosphate-based composites as injectable bone substitute materials. *J. Biomed. Mater. Res. Part B Appl. Biomater.* **2010**, *94*, 273–286. [[CrossRef](#)]
21. Ginebra, M.P.; Traykova, T.; Planell, J.A. Calcium phosphate cements as bone drug delivery systems: A review. *J. Control. Release* **2006**, *113*, 102–110. [[CrossRef](#)]
22. Zhang, J.; Liu, W.; Schnitzler, V.; Tancret, F.; Bouler, J.M. Calcium phosphate cements for bone substitution: Chemistry, handling and mechanical properties. *Acta Biomater.* **2014**, *10*, 1035–1049. [[CrossRef](#)]
23. O'Neill, R.; McCarthy, H.O.; Montufar, E.B.; Ginebra, M.P.; Wilson, D.I.; Lennon, A.; Dunne, N. Critical review: Injectability of calcium phosphate pastes and cements. *Acta Biomater.* **2017**, *50*, 1–19. [[CrossRef](#)]
24. Chow, L.C.; Eanes, E.D. Calcium phosphate cements. *Monogr. Oral Sci.* **2001**, *18*, 148–163.
25. Komath, M.; Varma, H.K. Development of a fully injectable calcium phosphate cement for orthopedic and dental applications. *Bull. Mater. Sci.* **2003**, *26*, 415–422. [[CrossRef](#)]
26. Ducheyne, P.; Hastings, G.W. *Metal and Ceramic Biomaterials*; CRC Press: Boca Raton, FL, USA, 1984; p. 31.
27. Sharpe, J.R.; Sammons, R.L.; Marquis, P.M. Effect of pH on protein adsorption to hydroxyapatite and tricalcium phosphate ceramics. *Biomaterials* **1997**, *18*, 471–476. [[CrossRef](#)] [[PubMed](#)]
28. Samavedi, S.; Whittington, A.R.; Goldstein, A.S. Calcium phosphate ceramics in bone tissue engineering: A review of properties and their influence on cell behavior. *Acta Biomater.* **2013**, *9*, 8037–8045. [[CrossRef](#)] [[PubMed](#)]
29. Uma Maheshwari, S.; Govindan, K.; Raja, M.; Raja, A.; Pravin, M.B.S.; Vasanth Kumar, S. Preliminary studies of PVA/PVP blends incorporated with HAp and β -TCP bone ceramic as template for hard tissue engineering. *Bio-Med. Mater. Eng.* **2017**, *28*, 401–415. [[CrossRef](#)] [[PubMed](#)]
30. Topsakal, A.; Ekren, N.; Kilic, O.; Oktar, F.N.; Mahirogullari, M.; Ozkan, O.; Sasmazel, H.T.; Turk, M.; Bogdan, L.M.; Stan, G.E.; et al. Synthesis and characterization of antibacterial drug loaded β -tricalcium phosphate powders for bone engineering applications. *J. Mater. Sci. Mater. Med.* **2020**, *31*, 1–17. [[CrossRef](#)]
31. Pan, Y.; Huang, J.L.; Shao, C.Y. Preparation of β -TCP with high thermal stability by solid reaction route. *J. Mater. Sci.* **2003**, *38*, 1049–1056. [[CrossRef](#)]
32. Bohner, M.; Santoni, B.L.G.; Döbelin, N. β -tricalcium phosphate for bone substitution: Synthesis and properties. *Acta Biomater.* **2020**, *113*, 23–41. [[CrossRef](#)]
33. Egli, P.S.; Müller, W.; Schenk, R.K. Porous hydroxyapatite and tricalcium phosphate cylinders with two different pore size ranges implanted in the cancellous bone of rabbits. A comparative histomorphometric and histologic study of bony ingrowth and implant substitution. *Clin. Orthop. Relat. Res.* **1988**, *232*, 127–138. [[CrossRef](#)]
34. Yamada, S.; Heymann, D.; Bouler, J.M.; Daculsi, G. Osteoclastic resorption of calcium phosphate ceramics with different hydroxyapatite/ β -tricalcium phosphate ratios. *Biomaterials* **1997**, *18*, 1037–1041. [[CrossRef](#)]
35. Kondo, N.; Ogoose, A.; Tokunaga, K.; Ito, T.; Arai, K.; Kudo, N.; Inoue, H.; Irie, H.; Endo, N. Bone formation and resorption of highly purified β -tricalcium phosphate in the rat femoral condyle. *Biomaterials* **2005**, *26*, 5600–5608. [[CrossRef](#)]
36. Zerbo, I.R.; Bronckers, A.L.; De Lange, G.; Burger, E.H. Localization of osteogenic and osteoclastic cells in porous β -tricalcium phosphate particles used for human maxillary sinus floor elevation. *Biomaterials* **2005**, *26*, 1445–1451. [[CrossRef](#)] [[PubMed](#)]
37. Abadi, M.B.H.; Ghasemi, I.; Khavandi, A.; Shokrgozar, M.A.; Farokhi, M.; Homaeigohar, S.S.; Eslamifar, A. Synthesis of nano β -TCP and the effects on the mechanical and biological properties of β -TCP/HDPE/UHMWPE nanocomposites. *Polym. Compos.* **2010**, *31*, 1745–1753. [[CrossRef](#)]
38. Yuan, H.; Fernandes, H.; Habibovic, P.; De Boer, J.; Barradas, A.M.; De Ruiter, A.; Walsh, W.R.; Van Blitterswijk, C.A.; De Bruijn, J.D. Osteoinductive ceramics as a synthetic alternative to autologous bone grafting. *Proc. Natl. Acad. Sci. USA* **2010**, *107*, 13614–13619. [[CrossRef](#)] [[PubMed](#)]
39. Tay, B.K.; Patel, V.V.; Bradford, D.S. Calcium sulfate- and calcium phosphate-based bone substitutes: Mimicry of the mineral phase of bone. *Orthop. Clin. N. Am.* **1999**, *30*, 615–623. [[CrossRef](#)]
40. Huan, Z.; Chang, J. Self-setting properties and in vitro bioactivity of calcium sulfate hemihydrate-tricalcium silicate composite bone cements. *Acta Biomater.* **2007**, *3*, 952–960. [[CrossRef](#)]
41. Cheng, K.; Zhu, W.; Weng, X.; Zhang, L.; Liu, Y.; Han, C.; Xia, W. Injectable tricalcium phosphate/calcium sulfate granule enhances bone repair by reversible setting reaction. *Biochem. Biophys. Res. Commun.* **2021**, *557*, 151–158. [[CrossRef](#)]
42. Podaropoulos, L.; Veis, A.A.; Papadimitriou, S.; Alexandridis, C.; Kalyvas, D. Bone regeneration using β -tricalcium phosphate in a calcium sulfate matrix. *J. Oral Implantol.* **2009**, *35*, 28–36. [[CrossRef](#)]
43. Teodorescu, M.; Bercea, M. Poly(vinylpyrrolidone)—A versatile polymer for biomedical and beyond medical applications. *Polym.-Plast. Technol. Eng.* **2015**, *54*, 923–943. [[CrossRef](#)]
44. Muppalaneni, S.; Omidian, H. Polyvinyl alcohol in medicine and pharmacy: A perspective. *J. Dev. Drugs* **2013**, *2*, 1–5. [[CrossRef](#)]
45. Tonsuaadu, K.; Gross, K.A.; Plüdüma, L.; Veiderma, M. A review on the thermal stability of calcium apatites. *J. Therm. Anal. Calorim.* **2012**, *110*, 647–659. [[CrossRef](#)]
46. Zidan, H.M.; Abdelrazek, E.M.; Abdelghany, A.M.; Tarabiah, A.E. Characterization and some physical studies of PVA/PVP filled with MWCNTs. *J. Mater. Res. Technol.* **2019**, *8*, 904–913. [[CrossRef](#)]
47. Omkaram, I.; Chakradhar, R.S.; Rao, J.L. EPR, optical, infrared and Raman studies of VO^{2+} ions in polyvinylalcohol films. *Phys. B Condens. Matter* **2007**, *388*, 318–325. [[CrossRef](#)]

48. Abdelghany, A.M.; Abdelrazek, E.M.; Badr, S.I.; Morsi, M.A. Effect of gamma-irradiation on (PEO/PVP)/Au nanocomposite: Materials for electrochemical and optical applications. *Mater. Des.* **2016**, *97*, 532–543. [[CrossRef](#)]
49. Mondal, D.; Mollick, M.M.R.; Bhowmick, B.; Maity, D.; Bain, M.K.; Rana, D.; Mukhopadhyay, A.; Dana, K.; Chattopadhyay, D. Effect of poly (vinyl pyrrolidone) on the morphology and physical properties of poly (vinyl alcohol)/sodium montmorillonite nanocomposite films. *Prog. Nat. Sci. Mater. Int.* **2013**, *23*, 579–587. [[CrossRef](#)]
50. Elashmawi, I.S.; Baiet, H.A. Spectroscopic studies of hydroxyapatite in PVP/PVA polymeric matrix as biomaterial. *Curr. Appl. Phys.* **2012**, *12*, 141–146. [[CrossRef](#)]
51. Kupletskaya, N.B.; Kazitsyna, P.A. *Application of UV, IR, and NMR-Spectroscopy in Organic Chemistry*; High School: Moscow, Russia, 1971; pp. 214–234.
52. Nakamoto, K. *IR and Raman Spectra of Inorganic and Coordination Compounds*; High School: Moscow, Russia, 1991.
53. Sadykov, R.; Lytkina, D.; Stepanova, K.; Kurzina, I. Synthesis of Biocompatible Composite Material Based on Cryogels of Polyvinyl Alcohol and Calcium Phosphates. *Polymers* **2022**, *14*, 3420. [[CrossRef](#)]

Disclaimer/Publisher's Note: The statements, opinions and data contained in all publications are solely those of the individual author(s) and contributor(s) and not of MDPI and/or the editor(s). MDPI and/or the editor(s) disclaim responsibility for any injury to people or property resulting from any ideas, methods, instructions or products referred to in the content.